

Minimizing Data Distortion of Periodically Reporting IoT Devices with Energy Harvesting

Chiara Pielli*, Čedomir Stefanović†, Petar Popovski† and Michele Zorzi*

*Department of Information Engineering, University of Padova, Padova, Italy

†Department of Electronic Systems, Aalborg University, Aalborg, Denmark

Email: piellich@dei.unipd.it, cs@es.aau.dk, petarp@es.aau.dk, zorzi@dei.unipd.it

Abstract—Energy harvesting is a promising technology for the Internet of Things (IoT) towards the goal of self-sustainability of the involved devices. However, the intermittent and unreliable nature of the harvested energy demands an intelligent management of devices' operation in order to ensure a sustained performance of the IoT application. In this work, we address the problem of maximizing the quality of the reported data under the constraints of energy harvesting, energy consumption and communication channel impairments. Specifically, we propose an energy-aware joint source-channel coding scheme that minimizes the expected data distortion, for realistic models of energy generation and of the energy spent by the device to process the data, when the communication is performed over a Rayleigh fading channel. The performance of the scheme is optimized by means of a Markov Decision Process framework.

I. INTRODUCTION

A lion's share of IoT applications involves scenarios in which a multitude of devices, i.e., sensors, periodically report a small amount of data about some monitored phenomena. A major challenge in this regard is to ensure uninterrupted service with minimal device maintenance. Specifically, a typical IoT device is expected to operate for very long periods without human intervention, achieving a minimum of 10 years of battery (i.e., device) operation in such IoT applications [1]–[3]. Energy Harvesting (EH) is a promising technology that can foster the required self-sustainability of the devices and, thus, of the IoT applications.

On the other hand, the EH process is stochastic in nature, requiring rethinking and redesign of the operation with respect to standard approaches employed for battery-operated devices. Specifically, in this work we consider a monitoring application where a sensor node powered by renewable energy sources periodically sends its measurements to a data gathering point. Before transmission, it performs processing operations, e.g., lossy joint source-channel coding that maximizes the reconstruction fidelity at the receiver, under the constraints imposed by the EH process. In particular, the reconstruction fidelity depends on the tradeoff between source compression accuracy and robustness against the channel impairments, and is represented in terms of data distortion.

The effect of packet losses on data distortion in standard communication scenarios, where there are no energy constraints, has already been treated, e.g., in [4], where the authors investigate erasure and scalable codes for a Gaussian source. Several works (e.g., [5]) analyze layered transmission

schemes, where the source is coded in superimposed layers, and each layer successively refines the description of the previous one, but is transmitted with a higher coding rate (i.e., subject to larger outage probability). Often, the distortion exponent is adopted as the performance metric for the end-to-end distortion [6], [7]. Nevertheless, the distortion exponent is meaningful only for the high SNR regime, which is not dominant in IoT scenarios.

A general overview of recent advances in wireless communications with EH is presented in [8]. Further, distortion minimization for EH sensor nodes has been studied in several works. In [9], the tradeoff between quantization and transmission energy in the presence of EH is analyzed, but the effect of packet losses on the received data quality is not taken into account. The problem of energy allocation between processing and transmission is also studied in [10], in a model similar to our own, but where, rather than minimizing the long-term distortion, the authors aim at guaranteeing a minimum average distortion while maintaining the data queue stable. In [11], the authors study the achievable distortion when the energy buffer may have some leakage and the transmitting devices jointly perform source-channel coding in the presence of Gaussian and binary sources.

The work closest to ours can be found in [12], where a sensor node employs an *on-line* transmission policy that maximizes the long-term average quality of the transmitted packets. Specifically, the transmitter can decide the degree of lossy compression and the transmission power, and the optimal transmission strategy is obtained through the use of Markov Decision Processes (MDPs). The framework employed in this paper bears similarities to the one from [12], with the following important differences: (i) in addition to source coding, we also consider channel coding, leveraging on the results of finite-length information theory; (ii) we do not perform power control, which requires Channel State Information (CSI) at the transmitter and thus implies an additional cost or overhead, and may be available only with a delay; and (iii) the actual distortion at the receiver is influenced not only by the source processing procedure, but also by the channel outage probability.

The problem considered in the paper is solved through decomposition into two nested optimization processes that respectively address the rate-distortion tradeoff and the energy management. A similar approach has been followed in [13], where the goal is to guarantee energy self-sufficiency to a

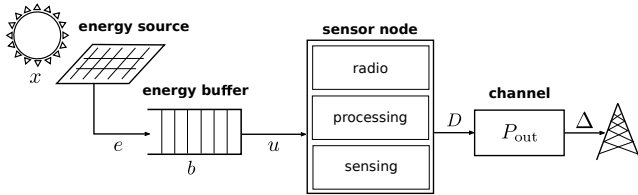


Figure 1: System model.

multi-hop network by adapting the nodes' duty cycle and the information generation rate. Again, the framework is modeled by means of an MDP; in fact MDPs are widely used to address energy management policies, because they represent an appealing solution to optimize some long-term utilities in the presence of stochastic EH [14]. The nested optimization allows us to determine an online optimal policy: although solving an MDP may require some computational time, the optimal solution can be precomputed and stored, such that during its operation the node decides on its action with a simple table look-up. We also note that the considered framework is based on realistic models of the EH process and of the distortion achievable by compressing environmental signals with practical algorithms, including a thorough energy consumption model.

The rest of the paper is organized as follows. The system model and the problem formulation are described in Sections II and III, respectively. The rate-distortion tradeoff is analyzed in Section IV, whereas Section V studies the energy management policy. Finally, we provide and discuss some exemplary numerical results in Section VI and draw the conclusions in Section VII.

II. SYSTEM MODEL

We consider an IoT device that generates packets periodically and communicates wirelessly with a data collector. Time is divided into slots of predefined duration T . Each time the device generates a packet, it has access to a slot reserved for its transmission. In terms of the classification from [8], the considered scenario can be categorized as an on-line energy management with a reward maximization and with a perfect knowledge of the state of the energy buffer, for a single device case.

Fig. 1 shows the dynamics of the sensor node: some energy-scavenging circuitry allows the device to harvest energy, which is stored in a buffer and used for sensing, processing and transmission operations. In the following, we thoroughly describe all the components of such model.

A. Data Processing and Transmission Model

The sensor node periodically senses the surrounding environment. In each time slot the device collects a constant number of readings for a total data size of L_0 bits per slot. In the following, we consider a typical slot when defining quantities of interest; in general, we will introduce subscripts referring to slots only when needed. The sensor node may exploit source coding; in particular, we consider lossy compression algorithms, and the resulting packet size after compression is $L(k) = k/m L_0$, where $m \in \mathbb{N}$, $k \in \{0, 1, \dots, m\}$. The

device decides upon k and thus on the compression ratio $k/m \in [0, 1]$. Lossy compression reduces the volume of bits of information to send, but at the cost of a poorer accuracy in the signal representation, as it introduces a distortion $D(k)$ that depends on the compression ratio.

The slot duration T defines the maximum number of bits that can fit into a slot, namely $S = T/T_b$, where T_b is the (fixed) bit duration. Hence, when deciding upon the degree of source compression k , the device also selects the coding rate $R(k) = L(k)/S$ at the same time. We assume that no CSI is available at the transmitter, which, therefore, does not perform power control and, whenever transmitting, uses a constant transmission power P_{tx} . Depending on $R(k)$ and on the actual channel conditions, the packet may not be correctly received with an outage probability $P_{out}(k)$. Since we consider a monitoring scenario where the traffic pattern is reasonably known in advance, we assume that the slot duration is allotted in such a way that the device can send all the gathered information within the slot, thus $L_0 \leq S$.

Both the distortion function and the outage probability will be characterized in Section IV.

B. Energy Harvesting Model

We assume that the device is capable of collecting energy from the environment, and that this energy supply exhibits time correlation. Our approach follows the works based on realistic data [15], [16] that assess the goodness of Markov Chains (MCs) to model time-dependent sources.

The energy source dynamics are modeled by means of a 2-state MC, and the number e_n of energy quanta harvested in slot n depends on the source state $x_n \in \mathcal{X} = \{0, 1\}$. Based on the realistic model of [16], we assume that, when $x_n = 0$, the source is in a "bad" state and $e_n = 0$ with probability 1, otherwise, the source is in a "good" state and the energy inflow follows a truncated discrete normal distribution, i.e., $e_n \sim \mathcal{N}(\mu, \sigma^2)$ in the discrete interval $\{1, \dots, E\}$.

We consider a *harvest-store-use* protocol: the energy scavenged in slot n is first stored in a battery of finite size B and then used from slot $n+1$ onwards. In slot n , the battery state is $b_n \in \{0, \dots, B\}$, and evolves as follows:

$$b_{n+1} = \min \{b_n + e_n - u_n, B\} \triangleq (b_n + e_n - u_n)^{\dagger}, \quad (1)$$

where $u_n \geq 0$ is the energy used in slot n . The energy causality principle entails that:

$$u_n \leq b_n \quad (2)$$

in all slots. We assume that the sensor node can reliably estimate the status of its energy buffer.

C. Energy Consumption Model

We consider the following sources of energy consumption.

Data processing. To model the energy consumed by compression, we leverage on the results of [17], where the authors map the number of arithmetic operations required to process the original signal into the corresponding energy demand:

$$E_P(k) = \begin{cases} E_0 L_0 N_P(k) & \text{if } 1 \leq k \leq m-1 \\ 0 & \text{if } k = 0, m \end{cases} \quad (3)$$

where E_0 models the energy spent by the micro-controller of the node in a clock cycle, and $N_P(k)$ is the number of clock cycles required by the compression algorithm per uncompressed bit of the input signal, which depends on the compression ratio. If the packet is not compressed ($k = m$) or discarded ($k = 0$), no energy is consumed.

Different compression algorithms entail different shapes of $N_P(k)$. In particular, there are some techniques for which function $N_P(k)$ is increasing and concave in k^1 , e.g., the Lightweight Temporal Compression (LTC) and the Fourier-based Low Pass Filter (DCT-LPF) algorithms. We consider the LTC algorithm, whose corresponding energy consumption turns out to be linear in the compression ratio: $N_P(k) = \alpha_P \frac{k}{m} + \beta_P$, $k \in \{1, \dots, m-1\}$, with $\alpha_P, \beta_P > 0$ [17].

Data transmission. The energy needed to transmit a signal with constant power P_{tx} for a time window of length T is:

$$E_{TX}(k) = \frac{P_{\text{tx}} T}{\eta_A} \cdot \chi_{\{k>0\}}, \quad (4)$$

where $\eta_A \in (0, 1]$ is a constant term that models the efficiency of the power amplifier of the antenna. The indicator function $\chi_{\{k>0\}}$, equal to 1 if $k > 0$ and to zero otherwise, ensures that no energy is consumed if the packet is discarded.

Other operations and circuitry costs. We define the circuitry energy consumption in a slot as:

$$E_C(k) = \beta_S + \beta_C + (\beta_E + \mathcal{E}_C T) \cdot \chi_{\{k>0\}}, \quad (5)$$

where β_S and β_E , respectively, represent the constant sensing and encoding costs, β_C accounts for switching between the node's operating modes and the maintenance of synchronization with the receiver, and the last term models the additional energy cost incurred by a transmission, where \mathcal{E}_C is a circuitry energy rate. We highlight that, typically, the energy demanded by the channel encoding procedure is so small as to be negligible.

The total energy consumption of the node is given by the sum of the contributions of Eqs. (3)-(5):

$$E_{\text{used}}(k) = E_P(k) + E_{TX}(k) + E_C(k), \quad (6)$$

which depends solely on k .

III. PROBLEM FORMULATION

Our goal is to minimize the long-term average distortion of the data transmitted by the sensor node while guaranteeing the self-sufficiency of the network. The optimal distortion point is selected according to a joint source-channel coding policy: the node has to choose the number of bits per symbol to transmit, which implies to decide both the degree of lossy compression at the source and the error correction coding rate. The identification of such a working point is also driven by the energy dynamics: the node is powered through EH, hence the energy income is intermittent and erratic, and it is crucial to design an intelligent scheme to manage the available energy.

To deal with the two aspects of distortion and energy, we split the problem into two intertwined subproblems.

¹Although this may appear as a counterintuitive result, it is due to practical implementation details. We refer the reader to [17] for a detailed explanation.

- **Rate-Distortion Problem (RDP):** it focuses on the rate-distortion issue, and assumes to have a given amount of energy available to accomplish its goal. RDP will be discussed in Section IV.
- **Energy Management Problem (EMP):** this module dynamically decides the energy to use in each slot with the ultimate objective of ensuring long-term, uninterrupted operation. This problem will be formulated and solved in Section V.

The two subproblems are tightly coupled: RDP selects the optimal operating point on the rate-distortion curve as a function of the available energy, whereas EMP decides how this energy varies depending on the battery state and the statistical knowledge of the EH process. In this way, the node is assured to be self-sufficient in an energetic sense and, under this operating condition, the long-term average distortion is minimized. The combined problem is solved by means of an MDP, as described in Section V.

Notice that the separability of RDP and EMP in the overall optimization process leads to optimality because, once we decide the energy to be spent from the energy buffer, we focus on the QoS and choose the action that minimizes the distortion and the overall optimization is guaranteed by solving the MDP.

IV. RATE-DISTORTION ANALYSIS

In this section, we determine the optimal point in the rate-distortion tradeoff when the available energy budget is given. The actual distortion at the receiver is influenced by both the lossy compression performed at the source and the errors introduced by the channel. More specifically, we consider the packet to be completely lost when in outage, which corresponds to the maximum distortion level.

We first proceed to characterize the distortion due to source coding and the outage probability as a function of the rate, and then explain how to derive the solution of RDP.

A. Distortion due to compression

As described in Section II-A, in each slot the device can compress its readings through a lossy compression algorithm, thereby achieving a lower rate $R(k)$, but, at the same time, introducing a certain degree of distortion. In the literature, there exist closed-form expressions for the rate-distortion curves for idealized compression techniques operating on Gaussian information sources, but for practical algorithms such curves are generally obtained experimentally.

With the aim of modeling a more realistic scenario, we leveraged on the work in [17] to derive a mathematical fit of rate-distortion curves that were obtained experimentally:

$$D(k) = \begin{cases} b \left(\left(\frac{k}{m} \right)^{-a} - 1 \right) & \text{if } k > 0 \\ D_{\text{full}} & \text{if } k = 0, \end{cases} \quad (7)$$

where $b > 0$, $0 < a < 1$, and D_{full} is the maximum distortion, reached when the data is not even transmitted (extreme case of compression ratio equal to 0). Notice that (7) is a convex decreasing function of the compression ratio k/m .

B. Outage probability

We consider an erasure channel at the packet level, where the erasure probability depends on the rate $R(k)$ and the actual channel conditions. The communication channel is affected by both fading and Additive White Gaussian Noise (AWGN). We assume a quasi-static scenario, hence the fading coefficient H remains constant over the packet duration. The device does not perform power control and the transmission power is fixed to P_{tx} ; the Signal-to-Noise Ratio (SNR) γ at the receiver is:

$$\gamma = \frac{|H|^2 P_{\text{tx}}}{A^2 (d/d_0)^\eta N} \triangleq |H|^2 \bar{\gamma}, \quad (8)$$

where N is the noise power, and the term $A^2 (d/d_0)^\eta$ accounts for path loss and depends on the path-loss exponent η , the distance between transmitter and receiver d , and a path-loss coefficient $A = 4\pi d_0 f_0 / c$, where f_0 is the transmission frequency, c the speed of light, and d_0 a reference distance for the antenna far field.

When the channel is in a deep fade (i.e., $|H|$ is small), the packet is lost and a packet erasure (i.e., channel outage) occurs. In IoT scenarios where packets are likely to be short, the concepts of capacity and outage capacity of classic information theory are no longer applicable. Recently, Polyansky, Poor and Verdú [18] developed a finite-length information theory that revisits the classical concepts of capacity when packets have short size. In particular, they defined the *maximum coding rate* $R^*(S, \varepsilon)$ as the largest coding rate $L(k)/S$ for which there exists an encoder/decoder pair of packet length S whose error probability is not larger than ε . Although the derivation of $R^*(S, \varepsilon)$ is an NP-hard problem, tight bounds have been derived and, for quasi-static channels, the following approximation holds [19]:

$$R^*(S, \varepsilon) = C_\varepsilon + \mathcal{O}\left(\frac{\log_2 S}{S}\right), \quad (9)$$

where C_ε is the classical outage capacity for an error probability not larger than ε . This is a very useful result, because it legitimates the use of the quantity $\log_2(1 + \gamma)$ even in the finite-length regime [19]. Based on these considerations, we define the outage probability as:

$$P_{\text{out}}(k) = \Pr(\log_2(1 + \gamma) < R(k)). \quad (10)$$

We assume the fading to follow a Rayleigh distribution, i.e., the fading matrix H has i.i.d., zero-mean, unit-variance, complex Gaussian entries, and therefore the outage probability can be expressed as:

$$P_{\text{out}}(k) = 1 - e^{-(2^{R(k)} - 1)/\bar{\gamma}}, \quad (11)$$

The outage probability is non-decreasing in $R(k)$, and thus in k , being initially convex and then concave. Notice that it increases with the distance d from the receiver.

C. Optimal rate-distortion point

Given the amount of energy available u in the current slot, the device must decide how many bits of information k to transmit within a packet of fixed size S . This corresponds to jointly selecting the source compression ratio and the coding

rate. The degree of compression employed affects the quality of the information by introducing a source distortion that is non-increasing in k , see Eq. (7). On the other hand, the outage probability given in (11) is non-decreasing in k , and thus there is a tradeoff between $D(k)$ and $P_{\text{out}}(k)$. The *actual* distortion $\Delta(k)$ experienced by a packet at the receiver side is equal to $D(k)$ if the packet has been delivered, which happens with probability $1 - P_{\text{out}}(k)$, and is equal to D_{full} otherwise.

Based on the definition of $\Delta(k)$, we set up RDP as follows:

$$\text{RDP:} \quad k^* = \min_{k \in \{0, \dots, m\}} \mathbb{E}[\Delta(k)] \quad (12a)$$

subject to:

$$E_{\text{used}}(k) \leq u \quad (12b)$$

where the expected *overall* distortion at the receiver is:

$$\mathbb{E}[\Delta(k)] = D(k)(1 - P_{\text{out}}(k)) + D_{\text{full}} P_{\text{out}}(k). \quad (13)$$

The discrete nature of k makes it harder to solve RDP. We thus introduce the continuous variable $w \in [0, m]$ and then map it into $k \in \{0, \dots, m\}$. Also, we initially analyze the energy and distortion aspects of the problem separately: we determine a value k_E^* that solves the energy constraint (12b) and a value k_R^* that solves RDP when Constraint (12b) is neglected, and then we combine them to obtain k^* .

We now focus solely on Constraint (12b). When $u > 0$, since $E_{\text{used}}(\cdot)$ is non-decreasing in $w \in [0, m-1]$, there exists a point $w_E^*(u)$ that minimizes the gap between the consumed and the allocated energy, which either solves Constraint (12b) with equality², or is equal to $m-1$. Then, we choose $k_E^*(u)$ as $\lfloor w_E^*(u) \rfloor$. Instead, if no energy is allocated ($u = 0$), then $k_E^*(u) = 0$ and the packet is discarded. Finally, notice that $E_{\text{used}}(m) < E_{\text{used}}(k)$, $k \in \{1, \dots, m-1\}$ because no energy is spent for the processing operations. We will see later how to include this case in the solution of RDP.

We now discuss how to determine k_R^* , and present the following key result.

Theorem 1. *If $L_0 \leq S$, the expected overall distortion $\mathbb{E}[\Delta(w)]$ has exactly one local minimum at w_R^* in the continuous interval $[0, m]$.*

Proof. See Appendix A. \square

There exists no closed-form for w_R^* (see the computation in Appendix A); however, it is easy to numerically determine it by means of dichotomic search over a restricted subinterval of $[0, m]$ and then derive its discrete counterpart k_R^* accordingly. We refer the reader to Appendix B for details.

Based on these observations, the optimal $k^*(u)$ is given by:

$$k^*(u) = \begin{cases} \min\{k_R^*, k_E^*(u)\} & \text{if } k_R^* < m \\ m \cdot \chi_{\{E_{\text{used}}(m) \leq u\}} & \text{if } k_R^* = m \end{cases} \quad (14)$$

Intuitively, the energy constraint (12b) does not allow to choose any $k > k_E^*(u)$. On the other hand, it is not efficient

²If $E_P(w)$ is not strictly increasing in w , multiple rates may satisfy Constraint (12b) with equality. In this case, we select the maximum of these values.

to use any $k > k_R^*$ even if possible, because it would lead to a worse expected distortion. When the joint source-channel coding optimization leads to $k_R^* = m$, the packet is sent without being compressed, given that there is enough energy to perform the transmission. Notice that, because of how $k^*(u)$ is defined, the expected distortion at the receiver $\mathbb{E}[\Delta(k^*(u))]$ is a non-increasing and convex function of u ; see Appendix A for details about convexity.

V. ENERGY MANAGEMENT

Through Eq. (14), RDP dictates the optimal coding rate $R^*(u_n) \triangleq L(k^*(u_n))/m$ when the energy u_n available in slot n is given. The allocation of u_n is influenced by the dynamics of the energy inflow and by the battery state, which have been characterized in Section II-B. In this section, we formulate the distortion-energy problem as an MDP, which is solved by means of the well-known Value-Iteration Algorithm (VIA) [20].

A. Formulation of the Markov Decision Process

We model the problem as an MDP defined by the tuple $(\mathcal{S}, \mathcal{U}, P, c(\cdot))$, with the components described as follows.

- $\mathcal{S} \triangleq \mathcal{X} \times \mathcal{B}$ is the system state space, where $\mathcal{X} = \{0, 1\}$ denotes the set of energy source states, and $\mathcal{B} = \{0, \dots, B\}$ represents the set of energy buffer states.
- \mathcal{U} is the action set. In each slot, the device observes the current system state s_n and chooses the amount of energy $u_n \in \mathcal{U}$ to use. This decision influences the joint source-channel coding scheme to adopt, as dictated by RDP through Eq. (14). The set of admissible actions in state $s \in \mathcal{S}$ is $\mathcal{U}_s \subseteq \mathcal{U}$. According to Eq. (2), the usable energy is constrained by the present charge of the battery, thus $\mathcal{U}_{s_n} = \{0, \dots, b_n\}$.
- P represents the transition probabilities that govern the system dynamics. In particular, the probability of going from state $s_n = (x_n, b_n)$ to $s_{n+1} = (x_{n+1}, b_{n+1})$ when the action taken is u_n is given by:

$$\Pr(s_{n+1}|s_n, u_n) = p_e(e_n|x_n) \cdot p_x(x_{n+1}|x_n) \cdot \delta(b_{n+1} - (b_n + e_n - u_n)^\dagger) \quad (15)$$

where $p_x(x_{n+1}|x_n)$ is obtained from the transition probability matrix of the MC that models the source state, $p_e(e_n|x_n)$ is the mass distribution function of the energy inflow in state x_n (see Section II-B), and $\delta(\cdot)$ is equal to one if the argument is zero, and zero otherwise. This last term is needed to ensure that the transitions between states are consistent with the dynamics of the battery state as determined by both the energy harvesting process and the transmission decisions.

- Finally, $c(\cdot)$ is the cost function. Because our goal is to minimize the distortion that affects the received packet, the cost in slot n is a positive quantity defined as:

$$c(s_n, u_n) = \mathbb{E}[\Delta(k^*(u_n))], \quad (16)$$

where $k^*(u_n)$ is the result of the optimization of RDP. Notice that, apparently, the cost depends solely on the

chosen action and not on the current state $s_n = (x_n, b_n)$. However, the action must be selected in set \mathcal{U}_{s_n} , which does depend on the present battery status b_n .

We aim at identifying a policy π , i.e., a sequence of decision rules that map the system state into the action to take. As discussed in Section III, the goal is to minimize the long-term average distortion, i.e., the long-term average cost:

$$J^\pi = \lim_{N \rightarrow +\infty} \frac{1}{N} \mathbb{E}_s \left[\sum_{n=0}^{N-1} c(s_n, u_n) \right], \quad (17)$$

which depends on the chosen admissible policy π (that decides upon the action u). In general, it also depends on the initial state s_0 , but the MDP we defined has a unichain structure and bounded costs, thus the asymptotic behavior is independent of the initial state and it is sufficient to consider only Markov policies [21], i.e., those for which the decision rule depends only on the current state s_n and not on time n .

The goal of EMP is to determine $J^* = \min_{\pi \in \Phi} J^\pi$ and the corresponding optimal policy $\pi^* = \operatorname{argmin}_{\pi \in \Phi} J^\pi$, where Φ denotes the set of all stationary Markov policies.

B. Solution of EMP

J^* can be proved to satisfy Bellman's optimality equation [20], and thus our MDP can be solved, e.g., through the Relative Value-Iteration Algorithm (RVIA), a version of the VIA used for infinite-horizon average cost MDPs [20]. RVIA defines two functions J and Q that are iteratively updated starting from an initial estimate $J_0(\cdot)$, e.g., $J_0(s) = 0 \forall s \in \mathcal{S}$. In particular, the i -th iteration determines:

$$Q_i(s, u) = c(s, u) + \sum_{s' \in \mathcal{S}} \Pr(s'|s, u) J_{i-1}(s') \quad (18)$$

$$J_i(s) = \min_{u \in \mathcal{U}_s} Q_i(s, u), \quad (19)$$

In (18), the immediate cost $c(s, u)$ obtained in the current state s is summed with the expected optimal cost obtained from the next slot onwards, weighed according to the system dynamics. The convergence criterion is given by the span seminorm operator $sp(j) \triangleq \max(j) - \min(j)$ computed for $j = J_{i+1}(s) - J_i(s)$; the span seminorm guarantees that (19) is a contraction mapping, and thus the RVIA algorithm is assured to converge (for details about convergence, we refer the reader to [20]). We stop the iterative algorithm when $sp(\cdot) \leq \varepsilon$, for a chosen tolerance threshold ε . The optimal policy π^* is then determined by computing the optimal action to follow in each state $s \in \mathcal{S}$, i.e., $u^*(s) = \operatorname{argmin}_{u \in \mathcal{U}_s} Q_n(s, u)$, where n is the last iteration of RVIA, and has the following key property.

Theorem 2. *The optimal policy is non-decreasing in the energy buffer state b .*

Proof. See Appendix C. □

By taking into account the discrete nature of the system state, we have that the optimal policy has a threshold structure, which is an appealing property for storage and implementation on resource constrained nodes.

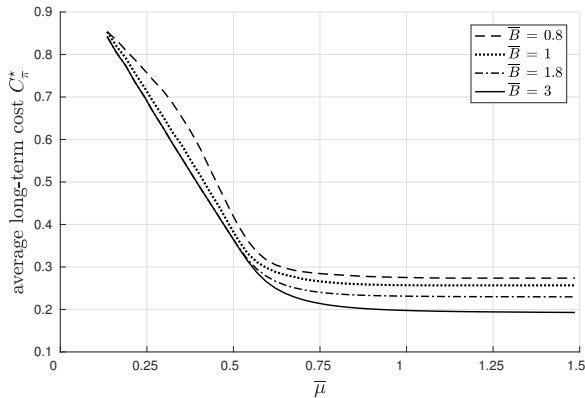


Figure 2: C_π^* vs $\bar{\mu}$ for different values of \bar{B} ($d = 100$ m).

When the optimal policy is identified, the MDP turns into a MC, and the average long-term cost induced by π^* is:

$$C_\pi^* = \sum_{s \in \mathcal{S}} \rho_s c(s, u^*(s)) \quad (20)$$

where ρ_s is the steady state probability of state s induced by the optimal policy, and $c(s, u^*(s))$ is the immediate cost obtained by following π^* in state s .

Note on computational complexity: We highlight that, although the determination of the optimal policy requires to solve the MDP, the RVIA algorithm does not need to be computed at runtime. As discussed, e.g. in [13], [22], the policy can be obtained offline and not necessarily by the sensor nodes, which will just need to store tables containing the association between system state and optimal action. Therefore, the policy execution simply consists in a look-up operation.

VI. NUMERICAL EVALUATION

To validate the analytical results, we evaluated the performance of the optimal policy by investigating the effect of some parameters and through comparison with two heuristics.

Concerning the processing aspects, we set $L_0 = S$, $a = 0.69$, $b = 3.27$, and $m = 20$. The channel gain is computed using the standard path loss model with a path loss exponent equal to 3.5 and a central frequency of 868.3 MHz. The bandwidth is $W = 125$ kHz, and the overall noise power is -167 dBm/Hz. For the energy aspect, the probability that the source goes from the bad to the good state is 3 times greater than that of the opposite transition. We set the variance of the normal distributed energy arrivals in the “good” state $\sigma^2 = 3$, whereas the mean μ will be specified for each result.

We introduce the following useful quantities: e_{\max} is the maximum energy consumption demanded by the processing and transmission of a packet, $\bar{\mu} = \mu/e_{\max}$, and $\bar{B} = B/e_{\max}$. We remark that, according to (6), a packet cannot be sent if the available energy is below a certain threshold e_{\min} .

Fig. 2 shows the average long-term cost C_π^* as a function of $\bar{\mu}$ for different values of \bar{B} , when the distance is fixed to 100 m. Clearly, the more the energy that can be harvested, the better the performance. It is interesting to note that, as long as it is sufficiently large, the battery size has only a minor impact on the average cost: when it is large enough to allow that k_R^* is reached in most of the time slots, it is not worth to

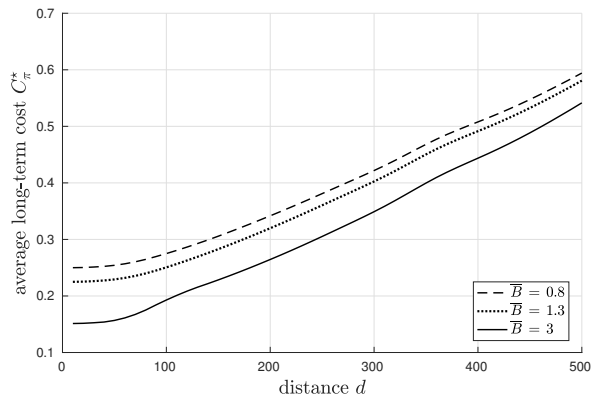


Figure 3: C_π^* vs d for different values of \bar{B} ($\bar{\mu} = 1$).

further increase B , because the exceeding energy is not used. Notice that, after a certain value of $\bar{\mu}$ (which depends on the other parameters), the average cost tends to stabilize around a specific configuration-dependent value. The reason behind it is twofold: (i) the distortion associated to k_R^* is never zero, unless the outage probability is negligible even for $k = m$ ³, and (ii) a minimum amount of energy is needed to transmit a packet and therefore, for all system states where the battery is $b < e_{\min}$, the cost is 0, and this has an impact on C^* , see Eq. (20).

Fig. 3 evaluates the performance of the optimal policy against the distance from the receiver for different values of the battery size when $\bar{\mu} = 1$. As d increases, the channel becomes worse and the higher outage probability has a negative impact on the achievable distortion at the receiver. Again, the role of B is less relevant.

A. Comparison with heuristics

We also compare the performance of the optimal policy (OP) against that of the two following heuristic policies.

- *Greedy policy (GP)*: the future sustainability of the node does not influence the energy to use in each slot, which is chosen as $u_n = \min(b_n, u^*)$, with u^* being the energy needed to achieve k_R^* . Basically, GP only solves RDP and does not optimize the energy utilization.
- *Dumb processing policy (DP)*: it does not determine the optimal point in the rate-distortion tradeoff and only considers the distortion introduced at the source, without accounting for the outage probability. EMP is unchanged.

Fig. 4 compares the performance of the optimal and heuristic policies against the average energy income during the good state of the energy source. The normalized battery size is $\bar{B} = 1.5$ and the distance from the receiver is $d = 80$ m. As expected, the optimal policy outperforms both heuristic policies. However, DP achieves almost optimal performance with this configuration: this is explained by the fact that the source distortion becomes flat as k increases (see (7)), thus the gain brought by OP for considering the negative impact of the outage probability is less significant than that of the

³We discarded this scenario, as it is not interesting. For $k < m$, it is always $\Delta(\cdot) \geq D(\cdot) > 0$.

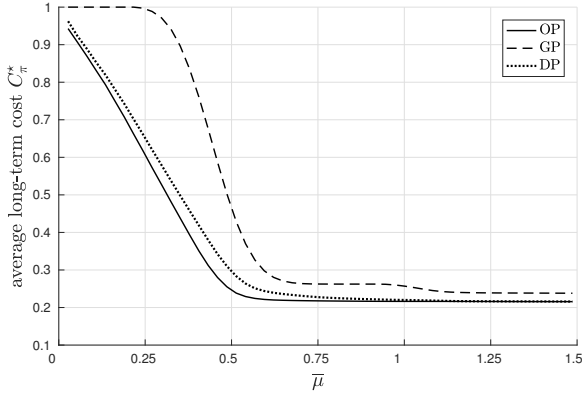


Figure 4: Performance comparison between policies.

intelligent energy management process⁴. In fact GP, that makes an aggressive use of the available energy, leads to the worst performance. When the average energy income μ is high, all policies achieve good performance, because there is almost always enough energy to guarantee low distortion.

In Fig. 5, we plot a realization of the system temporal evolution during the first 500 time slots, when $d = 80$ m and starting with full battery ($\bar{B} = 2$). The last graph shows the dynamics of the energy source, while the first three plots show the evolution of the energy buffer for OP, GP and DP, respectively. GP drains out the battery too fast, and the battery is often empty when $x_n = 0$, whereas this never happens with OP and DP, which leverage on the knowledge of the EH statistics to use the energy wisely. Interestingly, the excursion experienced by b_n is lower with DP than with OP: it neglects the negative impact of the outage probability for large values of k and tends to use energy to send the packet even when OP decides to discard it, and in this way it does not allow the buffer to accumulate energy that may be very useful in the next slots.

VII. CONCLUSIONS

This work investigates the tradeoff between energy efficiency and signal distortion at the receiver. We decomposed the problem into two nested optimization steps, endowing our framework with more flexibility. The outer problem is structured as an MDP, that allows to derive an optimal energy management policy; the inner problem jointly optimizes the source-channel coding scheme to ensure that the quality of the received information is maximized. The numerical evaluation corroborates the analytical results and shows that our policy outperforms simpler heuristics.

Future work includes the use of machine learning techniques in order to more accurately model the EH process and the extension to a sensor network where packet re-transmissions are allowed, thereby introducing a new tradeoff between signal distortion and transmission latency. We also would like to address more general cases, e.g., considering compression algorithms that behave differently from LTC in terms of energy consumption, and including practical sensor limitations, such as imprecisions in the energy buffer readings.

⁴Accordingly, if the outage were higher, the gap between DP and OP would increase.

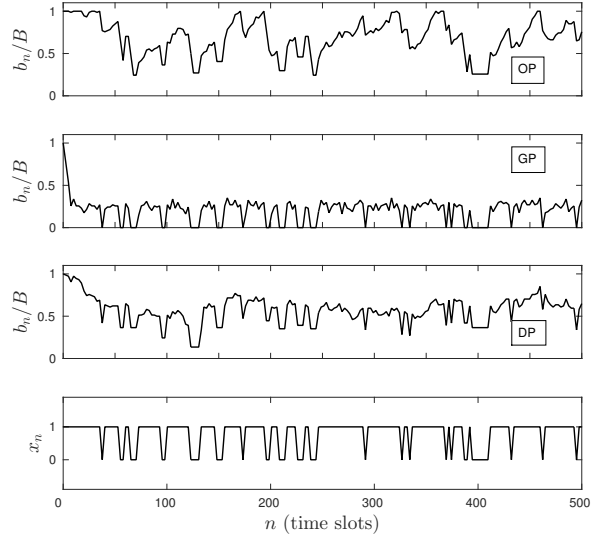


Figure 5: Example of battery temporal evolution ($\bar{B} = 2$).

ACKNOWLEDGMENTS

The work of C. Pielli and M. Zorzi was partly supported by Intel's Corporate Research Council, under the project "EC-CENTRIC: an energy- and context-centric optimization framework for IoT nodes". The work of Č. Stefanović was supported by the Danish Council for Independent Research under grant no. DFF-4005-00281.

APPENDIX A PROOF OF THEOREM 1

By substituting $D(\cdot)$ and $P_{\text{out}}(\cdot)$ in Eq. (12a) as given in Eqs. (7) and (11), respectively, the expected distortion for $w \in [1, m]$ is expressed as:

$$\mathbb{E}[\Delta(w)] = b \left(\left(\frac{w}{m} \right)^{-a} - 1 \right) e^{-\frac{2(wL_0)/(mS)-1}{\gamma}} + D_{\text{full}} \left(1 - e^{-\frac{2(wL_0)/(mS)-1}{\gamma}} \right) \leq D_{\text{full}}, \quad (21)$$

whereas it is equal to D_{full} for $w = 0$. By introducing the positive coefficients c_1, c_2, c_3, c_4 (given in Table I), Eq. (21) can be rewritten as:

$$\mathbb{E}[\Delta(w)] = c_1 w^{-a} e^{-c_2 2^{w c_3}} - c_4 e^{-c_2 2^{w c_3}} + D_{\text{full}}, \quad (22)$$

and its derivative with respect to w is:

$$\begin{aligned} \frac{\partial}{\partial w} \mathbb{E}[\Delta(w)] &= -e^{-c_2 2^{w c_3}} (d_1 w^{-a-1} + d_2 w^{-a} 2^{w c_3} - d_3 2^{w c_3}) \\ &\triangleq -e^{-c_2 2^{w c_3}} f(w), \end{aligned} \quad (23)$$

with positive coefficients d_1, d_2, d_3 detailed in Table I. The critical points of $\mathbb{E}[\Delta(w)]$ correspond to the zeros of $f(w)$. However, it is not possible to write a closed-form solution for $f(w) = 0$, but a numerical approach needs to be pursued.

Actually, the shape of $f(w)$ highly depends on coefficients d_1, d_2, d_3 , and thus on the system parameters. Anyway, we show that, if $L_0 \leq S$, $f(w)$ has at most one root in the continuous interval $[1, m]$, and thus function $\mathbb{E}[\Delta(w)]$ admits

c_1	c_2	c_3	c_4
$b m^a e^{1/\gamma}$	$1/\gamma$	$L_0/(mS)$	$e^{1/\gamma}(b + D_{\text{full}})$
d_1	d_2	d_3	d_4
$a c_1$	$c_1 c_2 c_3 \ln(2)$	$c_2 c_3 c_4 \ln(2)$	$e^{1/\gamma} c_2 c_3 \ln(2)$

Table I: Coefficients $c_1, c_2, c_3, c_4, d_1, d_2, d_3$.

a unique point of minimum w_R^* (which may coincide with one of the extreme values of w).

We temporarily focus only on the last two addends of $f(w)$ and define $g(w) \triangleq (d_2 w^{-a} - d_3) 2^{w c_3}$. By expanding coefficients d_2 and d_3 , we obtain:

$$g(w) = d_4 \left(b \left(\frac{m}{w} \right)^a - (b + D_{\text{full}}) \right) 2^{w c_3}, \quad (24)$$

with d_4 defined in Table I. The derivative is:

$$\begin{aligned} \frac{\partial}{\partial w} g(w) = & d_4 2^{w c_3} \left(-a b m^a w^{-a-1} + \right. \\ & \left. + b \left(\frac{m}{w} \right)^a \ln(2) c_3 - b \ln(2) c_3 - D_{\text{full}} \ln(2) c_3 \right) \end{aligned} \quad (25)$$

The last addend of the second factor is certainly negative, and the sum of the first three addends is equal to:

$$\begin{aligned} & b \left(\frac{m}{w} \right)^a \left(-\frac{a}{w} + \ln(2) c_3 \left(1 - \left(\frac{w}{m} \right)^a \right) \right) \leq \\ & \leq b \left(\frac{m}{w} \right)^a \left(-\frac{a}{w} + \frac{1}{m} \left(1 - \left(\frac{w}{m} \right)^a \right) \right) \triangleq b \frac{m^a}{w^a} h(w) \end{aligned} \quad (26)$$

where the first inequality comes from the assumption $L_0 \leq S$, that implies $c_3 \leq 1/m$. Notice that both $h(0)$ and $h(m)$ are negative, and $h'(w)$ is positive, i.e., function $h(\cdot)$ is a monotonically increasing negative function of $w \in [0, 1]$. It follows that, for $w \leq m$, $g(w)$ is always decreasing in w . Moreover, it is certainly positive for $w \rightarrow 0^+$ and negative for $w = m$. This means that $g(w)$ has exactly one point of minimum $w_g = (b/(b + D_{\text{full}}))^{1/a}$ in the continuous range $[0, m]$. However, if $w_g < 1$, then $g(w)$ is always negative in the interval we are interested in (i.e., $w \in [1, m]$).

Based on these observations and on the fact that $d_1 w^{-a-1}$ is positive, convex and decreasing in w , we obtain that $f(w)$ is decreasing in w . Depending on the values of d_1, d_2, d_3 , it is then possible to pinpoint three distinct cases.

- 1) $f(w)$ is always positive, and thus $\mathbb{E}[\Delta(w)]$ is always increasing in w , which entails that choosing $w_R^* = 1$ is optimal. This happens when coefficient d_1 is very high and thus the first addend of $f(w)$ always dominates $g(w)$, i.e., when the outage probability is overwhelming. We deem this case not to be of practical interest.
- 2) In contrast to the previous case, it may happen that $f(w)$ is always negative, i.e., $\mathbb{E}[\Delta(w)]$ always decreases with w . This situation is met when the distortion function prevails over the outage probability, which remains low even for high rates because the channel is very good on average. The solution in this case is $w_R^* = m$, i.e., the best strategy consists in not compressing at all.
- 3) Otherwise, $f(w)$ is decreasing in w and has a unique zero, which corresponds to a unique value w_R^* . Using a source compression ratio lower than w_R^*/m would generate a higher $\mathbb{E}[\Delta(\cdot)]$ because of the larger distortion introduced with the source coding, whereas a

compression ratio larger than w_R^*/m would weaken the goodness of the channel coding and lead to a higher outage probability.

In practice, under the only assumption of $L_0 \leq S$, there always exists a unique point w_R^* that minimizes the expected distortion at the receiver, i.e., $\mathbb{E}[\Delta(w)]$ is decreasing until w_R^* and increasing afterwards. \square

A note on convexity. $\mathbb{E}[\Delta(w)]$ is *convex* for $w \leq w_R^*$. In fact, the computation of the second derivative of (21) leads to:

$$\begin{aligned} \frac{\partial^2}{\partial w^2} \mathbb{E}[\Delta(w)] = & c_2 c_3 \ln(2) 2^{w c_3} e^{-c_2 2^{w c_3}} f(w) + \\ & - c_2 e^{-c_2 2^{w c_3}} \frac{\partial}{\partial w} f(w) \end{aligned} \quad (27)$$

which is always positive for $w \leq w_R^*$, since $f(w)$ is positive and its derivative $-(a+1)d_1 w^{-a-2} + \frac{\partial}{\partial w} g(w)$ is always negative.

APPENDIX B

ON THE DETERMINATION OF k_R^*

The computation in Appendix A shows that w_R^* cannot be expressed with a closed-form. So, in the worst case $\mathbb{E}[\Delta(k)]$ should be calculated for all the m possible values of k . However, it is still possible to determine k_R^* with the following procedure, that reduces the computational time. First of all, we compute the value of Eq. (21) for the two extreme values $k \in \{1, m\}$. If both $f(1)$ and $f(m)$ are positive, then we fall in case 1) of Appendix A and $k_R^* = 1$; similarly, if they are both negative, case 2) holds and $k_R^* = m$. If $f(1) > 0$ and $f(m) < 0$, case 3) holds and k_R^* can be found by means of binary search over the discrete subinterval $[k_g, m-1]$, where k_g is one of the two closest integers to w_g , according to which one yields the lowest expected distortion.

APPENDIX C

PROOF OF THEOREM 2

Thanks to Topkis' monotonicity theorem [23], to prove that $u^*(s) = \operatorname{argmin}_{u \in \mathcal{U}_s} Q((x, b), u)$ is non-decreasing in b , it is sufficient to prove that function $Q((x, b), u)$ is *submodular* in (b, u) , i.e., that the difference $Q((x, b), u') - Q((x, b), u)$ with $u' \geq u$ does not increase as b increases:

$$Q((x, b'), u') - Q((x, b'), u) \leq Q((x, b), u') - Q((x, b), u) \quad (28)$$

for $b' \geq b$. The submodularity property is preserved under non-negative linear combination, thus we separately demonstrate the submodularity of $c(s, u)$ and $J(s)$ in the pair (b, u) . In fact, from Eq. (19), we have that $Q((x, b), u) = c((x, b), u) + \sum_{x' \in \mathcal{X}} \sum_{e=0}^E p_x(x'|x) p_e(e|x) J((x', b+e-u))$.

For what concerns the single-stage cost $c((x, b), u)$, we have seen in Section IV-C that it is convex and non-increasing in u , and depends on b only through the set of admissible actions $\mathcal{U}_{(x,b)}$. Since $\mathcal{U}_{(x,b)} \subseteq \mathcal{U}_{(x,b')}$ if $b \leq b'$, it is $c((x, b), u) < c((x, b'), u)$ for $b < u \leq b'$, and $c((x, b), u) = c((x, b'), u)$ in all other cases. It follows that the quantity $c((x, b'), u) - c((x, b), u)$ does not increase as u increases, i.e., the single-stage cost is submodular in (b, u) .

We now proceed with the characterization of the term $J((x, b))$. We assume it to be convex in the energy buffer state b ; the validity of this property is proven in Lemma 1 below. Convexity means that:

$$J((x, b_1)) + J((x, b_2)) \geq J((x, \lambda b_1 + (1 - \lambda)b_2)) + J((x, (1 - \lambda)b_1 + \lambda b_2)) \quad (29)$$

for any $\lambda \in [0, 1]$, b_1, b_2, x . By choosing $b_1 = b + e - u'$, $b_2 = b' + e - u$, and $\lambda = (u' - u)/(u' - u + b' - b)$ with $b' \geq b$ and $u' \geq u$, and by rearranging the terms, we obtain:

$$J((x, b' + e - u')) - J((x, b' + e - u)) \leq J((x, b + e - u')) - J((x, b + e - u)), \quad (30)$$

which proves the submodularity of $J(x, b)$ in (b, u) .

Summing up, by exploiting the submodularity of function $Q((x, b), u)$ and the convexity of $J((x, b))$ with respect to b , we have proved that the optimal policy $\pi^*(s)$ is non-decreasing in the buffer state b .

Lemma 1. $J(s)$ is convex in the energy buffer state b .

Proof. We proceed by induction on the i -th iteration of RVIA (see Eq. (19)).

The basis is straightforward: since the initial value $J_0((x, b))$ does not affect the convergence of the algorithm, we simply choose it convex in b (e.g., $J_0((x, b)) = 0 \forall s \in \mathcal{S}$ is a valid choice).

For the inductive step, we assume $J_{i-1}((x, b))$ to be convex in b . In the proof of Theorem 2 we have shown that $Q(s, u)$ is submodular in b if $J((x, b))$ is convex in b , i.e.:

$$Q_i((x, b), u') - Q_i((x, b - c), u') \leq Q_i((x, b), u) - Q_i((x, b - c), u), \quad (31)$$

for $b' \geq b$, $u' \geq u$. Function $Q_i((x, b), u)$ is convex in b , because it is the nonnegative weighted sum of $c((x, b), u)$ and $J_{i-1}((x, b))$, that are both convex in b . Thus:

$$Q_i((x, b), u) - Q_i((x, b - c), u) \leq Q_i((x, b + c), u) - Q_i((x, b), u), \quad (32)$$

which, combined with (31), gives:

$$Q_i((x, b), u') - Q_i((x, b - c), u') \leq Q_i((x, b + c), u) - Q_i((x, b), u), \quad (33)$$

$$Q_i((x, b, u) - Q_i((x, b - c), u') \leq Q_i((x, b + c), u) - Q_i((x, b), u'). \quad (34)$$

By choosing $u = u' = \operatorname{argmin}_{\underline{u}} Q_i((x, b), \underline{u})$, we obtain:

$$J_i((x, b + c)) - J_i((x, b)) \geq J_i((x, b)) - J_i((x, b - c)), \quad (35)$$

i.e., $J_i(s)$ is convex in b and the inductive step is proved.

REFERENCES

- [1] Nokia. (2015) LTE evolution for IoT connectivity. [Online]. Available: <http://resources.alcatel-lucent.com/asset/200178>
- [2] Ericsson. (2015) Ericsson, AT&T and Altair demonstrate over 10 years of battery life on LTE IoT commercial chipset. [Online]. Available: <https://www.ericsson.com/news/1962068>
- [3] Huawei. (2015) NB-IOT - Enabling New Business Opportunities. [Online]. Available: <http://www.huawei.com/minisite/4-5g/img/NB-IOT.pdf>
- [4] K. E. Zachariadis, M. L. Honig, and A. K. Katsaggelos, "Source fidelity over fading channels: performance of erasure and scalable codes," *IEEE Transactions on Communications*, vol. 56, no. 7, pp. 1080–1091, July 2008.
- [5] F. Etemadi and H. Jafarkhani, "A unified framework for layered transmission over fading and packet erasure channels," *IEEE Transactions on Communications*, vol. 56, no. 4, pp. 565–573, Apr. 2008.
- [6] J. N. Laneman, E. Martinian, G. W. Wornell, and J. G. Apostolopoulos, "Source-channel diversity for parallel channels," *IEEE Transactions on Information Theory*, vol. 51, no. 10, pp. 3518–3539, Oct. 2005.
- [7] I. E. Aguerri and D. Gunduz, "Distortion exponent in fading MIMO channels with time-varying side information," in *2011 IEEE International Symposium on Information Theory Proceedings*, July 2011, pp. 548–552.
- [8] S. Ulukus, A. Yener, E. Erkip, O. Simeone, M. Zorzi, P. Grover, and K. Huang, "Energy harvesting wireless communications: A review of recent advances," *IEEE Journal on Selected Areas in Communications*, vol. 33, no. 3, pp. 360–381, Mar. 2015.
- [9] R. V. Bhat, M. Motani, and T. J. Lim, "Distortion minimization in energy harvesting sensor nodes with compression power constraints," in *2016 IEEE International Conference on Communications (ICC)*, May 2016, pp. 1–6.
- [10] P. Castiglione, O. Simeone, E. Erkip, and T. Zemen, "Energy management policies for energy-neutral source-channel coding," *IEEE Transactions on Communications*, vol. 60, no. 9, pp. 2668–2678, Sept. 2012.
- [11] M. S. Motlagh, M. B. Khuzani, and P. Mitran, "On lossy joint source-channel coding in energy harvesting communication systems," *IEEE Transactions on Communications*, vol. 63, no. 11, pp. 4433–4447, Nov. 2015.
- [12] D. Zordan, T. Melodia, and M. Rossi, "On the design of temporal compression strategies for energy harvesting sensor networks," *IEEE Transactions on Wireless Communications*, vol. 15, no. 2, pp. 1336–1352, Feb. 2016.
- [13] N. Bui and M. Rossi, "Staying alive: System design for self-sufficient sensor networks," *ACM Transactions on Sensor Networks*, vol. 11, no. 3, pp. 40:1–40:42, Feb. 2015.
- [14] M. L. Ku, W. Li, Y. Chen, and K. J. R. Liu, "Advances in energy harvesting communications: Past, present, and future challenges," *IEEE Communications Surveys Tutorials*, vol. 18, no. 2, pp. 1384–1412, Second Quarter 2016.
- [15] M. L. Ku, Y. Chen, and K. J. R. Liu, "Data-driven stochastic models and policies for energy harvesting sensor communications," *IEEE Journal on Selected Areas in Communications*, vol. 33, no. 8, pp. 1505–1520, Aug. 2015.
- [16] M. Miozzo, D. Zordan, P. Dini, and M. Rossi, "Solarstat: Modeling photovoltaic sources through stochastic markov processes," in *2014 IEEE International Energy Conference*, May 2014, pp. 688–695.
- [17] D. Zordan, B. Martinez, I. Vilajosana, and M. Rossi, "On the performance of lossy compression schemes for energy constrained sensor networking," *ACM Transactions on Sensor Networks*, vol. 11, no. 1, pp. 15:1–15:34, Nov. 2014.
- [18] Y. Polyanskiy, H. V. Poor, and S. Verdú, "Channel coding rate in the finite blocklength regime," *IEEE Transactions on Information Theory*, vol. 56, no. 5, pp. 2307–2359, May 2010.
- [19] W. Yang, G. Durisi, T. Koch, and Y. Polyanskiy, "Quasi-static multiple-antenna fading channels at finite blocklength," *IEEE Transactions on Information Theory*, vol. 60, no. 7, pp. 4232–4265, July 2014.
- [20] D. Bertsekas, *Dynamic Programming and Optimal Control*, 4th ed. Belmont, MA, USA: Athena Scientific, 2012, vol. 2.
- [21] E. Altman, *Constrained Markov decision processes*. CRC Press, 1999, vol. 7.
- [22] A. Aprem, C. R. Murthy, and N. B. Mehta, "Transmit power control policies for energy harvesting sensors with retransmissions," *IEEE Journal of Selected Topics in Signal Processing*, vol. 7, no. 5, pp. 895–906, Oct. 2013.
- [23] D. M. Topkis, *Supermodularity and complementarity*. Princeton University Press, 1998.